C. R. Palevol 15 (2016) 978–987

Contents lists available at ScienceDirect

Comptes Rendus Palevol

www.sciencedirect.com

Human Palaeontology and Prehistory (Paleoanthropology)

An Early Pleistocene human pedal phalanx from Swartkrans, SKX 16699, and the antiquity of the human lateral forefoot

Une phalange de pied humain du Pléistocène inférieur de Swartkrans, SKX 16699, et l'antiquité de la partie avant latérale du pied humain

Erik Trinkaus [a,*], Biren A. Patel [b,c,d]

[a] *Department of Anthropology, Washington University, Saint Louis, MO 63130, USA*
[b] *Department of Cell and Neurobiology, Keck School of Medicine, University of Southern California, Los Angeles, CA 90033, USA*
[c] *Human and Evolutionary Biology Section, Department of Biological Sciences, University of Southern California, Los Angeles, CA 90089, USA*
[d] *Evolutionary Studies Institute, University of the Witwatersrand, Wits, 2050 Johannesburg, South Africa*

ARTICLE INFO

Article history:
Received 23 June 2016
Accepted after revision 20 July 2016
Available online 9 September 2016

Handled by Roberto Macchiarelli

Keywords:
Paleoanthropology
Foot
Toes
Australopithecus
Paranthropus
Homo

ABSTRACT

In order to assess the antiquity of derived human lateral (lesser) toe morphology, the SKX 16699 Early Pleistocene pedal proximal phalanx from Swartkrans (South Africa) was compared to samples of pedal phalanges attributed to Pliocene/Pleistocene australopithecines, *Homo naledi* and Late Pleistocene *Homo*. In contrast to australopith lateral phalanges, the SKX 16699 phalanx exhibits an absolutely (and probably relatively) short length, limited plantar diaphyseal curvature, proximal-to-midshaft and mid-dorsoplantar flexor sheath insertions, and a marked proximodorsal orientation of the metatarsal facet. SKX 16699 is intermediate between the australopith phalanges and later *Homo* ones in its modest dorsal diaphyseal curvature and mid-dorsoplantar metatarsophalangeal collateral ligament insertion areas. Its diaphyseal robustness is similar to that of *Homo* phalanges, but overlaps the range of later australopith ones. This combination of features and the close morphological affinities of SKX 16699 to later *Homo* proximal pedal phalanges suggest the emergence of a distinctly human lateral forefoot by the initial Early Pleistocene.

Mots clés :
Paléoanthropologie
Pied
Orteils
Australopithecus
Paranthropus
Homo

RÉSUMÉ

L'antiquité de la morphologie latérale dérivée des orteils humains est mal connue, malgré la présence de phalanges proximales de pied parmi les restes fossiles des australopithèques et du genre *Homo*. Pour clarifier l'évolution humaine du pied disto-latéral, la phalange proximale de pied du Pléistocène inférieur de Swartkrans (Afrique du Sud), SKX 16699 est comparée aux phalanges proximales de pieds d'australopithèques, d'*Homo naledi*, et d'hommes du Pléistocène supérieur. Contrairement à celles des australopithèques, la

* Corresponding author. Department of Anthropology, Washington University, Saint Louis, MO 63130, USA.
E-mail address: trinkaus@wustl.edu (E. Trinkaus).

http://dx.doi.org/10.1016/j.crpv.2016.07.003
1631-0683/

phalange SKX 16699 montre une faible longueur (en valeur absolue et relative par rapport à la tête fémorale), une courbure plantaire de la diaphyse limitée, une orientation proximo-dorsale marquée de la facette métatarsienne et les insertions des ligaments pour la gaine du tendon fléchisseur proximales et médio-dorsoplantaires. La phalange SKX 16699 est morphologiquement intermédiaire entre celles des australopithèques et celle du genre *Homo* plus récent, en ce qui concerne sa courbure diaphysaire dorsale et la position médio-dorsoplantaire des insertions des ligaments collatéraux métatarsophalangiens. Sa robustesse diaphysaire est proche de celles des phalanges proximales du genre *Homo*, mais dépasse celle des phalanges des australopithèques. Cette combinaison d'aspects morphologiques et les proches affinités de SKX 16699 avec les phalanges proximales du pied du genre *Homo* plus récent impliquent un fonctionnement de la partie avant latérale du pied clairement humain au début du Pléistocène, quelle qu'ait été la mosaïque morpho-fonctionnelle du pied tarso-métatarsien et du gros orteil humain à la même période.

1. Introduction

Later Pleistocene and recent humans evolved pedal skeletons related to the absorption and transfer of ground reaction forces during our striding bipedal gait, combined with effective propulsion during heel-off and toe-off. Many of the key elements of this pedal anatomy, including an adducted hallux, medial and lateral longitudinal pedal arches, and a compact posterior tarsal region with a robust heel, had emerged in the australopithecines in the Early-to-Middle Pliocene, as reflected in their pedal remains and the Laetoli footprints (Crompton et al., 2012; DeSilva et al., 2013; Raichlen et al., 2010; Ward, 2013). However, the degree to which species of *Australopithecus* and *Paranthropus* possessed a fully "human" heel-off and toe-off mechanism remains uncertain (DeSilva et al., 2012; Hatala et al., 2016; Susman and de Ruiter, 2004). What is known is that the phalanges of the lesser (lateral, or non-hallucal) toes of *Australopithecus* retained a suite of features reminiscent of those of *Ardipithecus* (Lovejoy et al., 2009), as well as the Pliocene hominin foot from Burtele (BRT) (Haile-Selassie et al., 2012). In particular, the lateral pedal proximal phalanges of *Australopithecus afarensis* were relatively long and gracile, dorsally curved, had prominent and distally positioned flexor sheath attachments, and exhibited other features in contrast to those of recent humans (Duncan et al., 1994; Latimer et al., 1982; Susman et al., 1984; Ward et al., 2012). The more recent australopithecine pedal phalanges, StW 355 from Member 4 of Sterkfontein and DNH-117 from Drimolen, largely follow the same pattern (Vernon, 2013).

Relatively short intermediate and distal lateral pedal phalanges are known from the KNM-ER 803 early *Homo* partial skeleton (Day and Leakey, 1974), and a partial lateral pedal proximal phalanx (ATD6-32) is known from the terminal Early Pleistocene (Lorenzo et al., 1999); they provide little information on when the later human lateral forefoot morphological pattern emerged. A number of lateral pedal proximal phalanges come from the Middle Pleistocene Atapuerca SH sample, and they provide a morphology well within the variation of Late Pleistocene and recent humans (Pablos et al., 2015). Although the recently discovered Dinaledi (*Homo naledi*) sample provides a distinctly human tarsometatarsal skeleton, its lateral pedal proximal phalanges have been described as having a mixture of australopith and later human features (Harcourt-Smith et al., 2015). Unfortunately, secure dates for this sample remain elusive (Dembo et al., 2016). It therefore remains unclear when the full morphology of the human lateral forefoot emerged.

In this context, we reassess a complete, but isolated, lateral hominin pedal proximal phalanx (SKX 16699) from the initial Early Pleistocene (≈1.8 Ma) of Swartkrans, South Africa (Susman et al., 2001) (Fig. 1). Its preliminary description emphasized the specimen's diminutive size, and highlighted its minimal diaphyseal curvature, dorsally "excavated" metatarsal facet, well-developed metatarsophalangeal ligament attachments, and "hourglass" shape, all features principally seen in more recent *Homo* pedal phalanges. Re-assessment of SKX 16699 in light of an expanded sample of fossil hominin pedal phalanges is therefore warranted and provides additional perspectives on the evolutionary timing of human-like lateral forefoot morphology.

2. Materials and methods

2.1. SKX 16699 pedal phalanx

The SKX 16699 phalanx (Fig. 1) is a complete pedal phalanx, with minimal erosion to its proximal and distal ends. It was associated with sediments from the Lower Bank of Member 1 of the Swartkrans deposits and thus dates to ≈1.8 Ma (Balter et al., 2008). It is likely to be from the right side based a lateral orientation (7°) of the distal trochlea. A right side designation is further supported by a small tubercle just distal of the proximal capsular attachment on the right side in dorsal view. If this tubercle represents the insertion of the abductor digiti minimi tendon, it would be from the fifth digit. Yet, the proximal epiphysis is virtually round (breadth/height ratio of 1.03 [1.01 with the extra plantar growth – see below]), which places it below the same ratio for all other Pliocene and Pleistocene hominin fifth proximal phalanges (1.07–1.34; $n = 22$) but within the range of second to fourth ones (0.89–1.28; $n = 93$). The tubercle could be for the tendon of the third or fourth dorsal

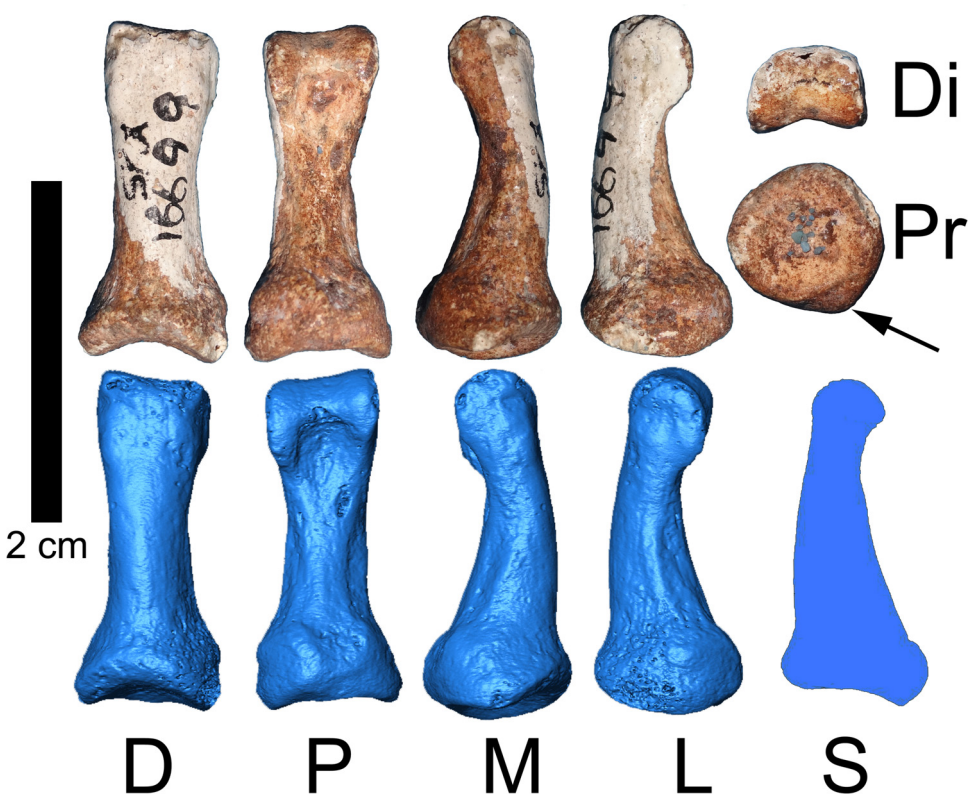

Fig. 1. The SKX 16699 proximal pedal phalanx in dorsal (D), plantar (P), medial (M), lateral (L), distal (Di) and proximal (Pr) views, photos (above) and 3D renderings from micro-CT scan images (below), plus the mid-sagittal section of the bone (S). The extra plantar-lateral bone on the proximal epiphysis is evident in the proximal view (arrow).
Fig. 1. Phalange proximale latérale du pied SKX 16699 en vues dorsale (D), plantaire (P), médiale (M), latérale (L), distale (Di) et proximale (Pr). Les photos (en haut) et les images micro-CT 3D (en bas) proviennent de la phalange, avec une section médio-sagittale (S). L'os supplémentaire sur la partie plantaire latérale de l'épiphyse proximale est indiqué sur la vue proximale (flèche).

interosseus muscle, but it is unlikely to be from the second one given the absence of a medial proximal tubercle for the first dorsal interosseus tendon. The phalanx is therefore most likely from the third, fourth or fifth digit.

There is a small bulge on the lateral side of the plantar proximal epiphysis, which has a slightly irregular and discrete border (Fig. 1). It is a small growth of bone, associated with the lateral plantar ligament, but expanded beyond the usual small tubercle for the ligament. The proximal maximum height has been adjusted (from 8.8 to 8.6 mm) to account for this extra growth.

2.2. Comparative samples

The SKX 16699 phalanx is qualitatively and quantitatively compared to samples of proximal lateral pedal phalanges of (frequently shod) Upper Paleolithic modern humans ($n = 80$), habitually unshod Middle Paleolithic early modern and late archaic humans ($n = 85$), the Dinaledi (*H. naledi*) sample ($n = 9$), and australopith ($n = 18$) remains referred to *Australopithecus afarensis*, *Australopithecus africanus* and *Paranthropus robustus*, plus the taxonomically uncertain Burtele Pliocene foot (BRT-VP-2/73) (the individual specimens are listed in Table S1). The *Australopithecus afarensis* phalanges are from Hadar (one from A.L. 288-1y, four from A.L. 333-115, and seven isolated ones from the A.L. 333 locality). The *Australopithecus africanus* and *P. robustus* phalanges are from Sterkfontein (StW 355) and Drimolen (DNH-117), respectively. Phalanges from digits 2 to 5 are included, given the difficulties in assigning isolated ones to digits 2 to 4. Recent human reference data for diaphyseal robusticity are from the habitually unshod Pecos Pueblo, New Mexico late prehistoric Amerindian sample (Trinkaus, 2005). The SKX 16699, StW 355, most Late Pleistocene and Holocene data are from personal measurement of the original specimens. The other phalangeal data derive from the literature and personal communications (Table S1).

2.3. Comparative methods

The assessment of SKX 16699 (Fig. 1) is based on the original specimen housed in the Ditsong National Museum of Natural History (Pretoria, South Africa), combined with high-resolution micro-CT scans (23.5 μm voxel resolution) of the bone obtained with a Nikon Metrology XTH 225/320 LC dual source industrial CT system located at the Microfocus X-ray CT facility of the University of the Witwatersrand. The lengths and diameters (Table S1) were measured with calipers (and verified on the digital scan data) following

Trinkaus (1983). An 'articular angle' was measured in the midline parasagittal plane of the phalanx, between the tangent to the metatarsal facet and the interarticular axis of the phalanx (Fig. S1); a proximodorsal orientation of the facet provides an angle > 90°. This angle is modestly less than the more commonly measured angle between the metatarsal facet and the plantar plane of the phalanx (i.e., the 'dorsal canting' angle; Duncan et al., 1994; Haile-Selassie et al., 2012; Ward et al., 2012). The articular angle better represents the functional (joint reaction force) orientation of the proximal phalanx in the latter portions of stance phase, given the dorsiflexion of the metatarsophalangeal joint and the associated plantarflexion of the interphalangeal joints at heel-off (Martin, 2011). Published 'dorsal canting' angles have been converted to 'articular angles' by subtracting the angles, in lateral view, between the plantar tangent and the interarticular axis from the available 'dorsal canting' angles (Fig. S1). All of these angles are likely to have measurements errors of ± 1°–2°, given irregularities in the articular facet margins unrelated to the predominant orientations of the facets.

Given differences in *Australopithecus* versus *Homo* in relative toe lengths (Latimer and Lovejoy, 1990; Susman et al., 1984; White and Suwa, 1987), relative phalanx length was assessed using an index of phalangeal length to available femoral head diameters (see Table S2 for Pliocene and Early Pleistocene femoral head diameters). Femoral head diameter is employed as a reflection of body mass (Auerbach and Ruff, 2004); it scales similarly across Pliocene and Early/Middle Pleistocene hominin samples to other skeletal reflections of body mass, and it is insignificantly proportionately smaller in the earlier samples than it is among Late Pleistocene and recent humans (Grabowski et al., 2015; Trinkaus, unpub. data). Associated femoral head diameters are used as available for A.L. 288-1 and the Late Pleistocene *Homo* phalanx samples. An average of 37.4 mm (± 4.1 mm; from A.L. 152-2, 333-3 and 827-1) is used for the other *Australopithecus afarensis* phalanges (data from Ward et al., 2012). A mean *Australopithecus africanus* value of 33.2 mm (± 2.4 mm, $n = 7$) is used for StW 355, and a mean *P. robustus* value of 32.2 mm (± 3.3 mm, $n = 6$) is employed for DNH-117 (data from Ruff, 2010). The *H. naledi* lengths are compared to the mean of the two available femoral head diameters (35.5 mm) (Marchi et al., 2016). SKX 16699 is compared to both the *P. robustus* mean and an early *Homo* average of 42.8 mm (± 3.3 mm, $n = 4$; data from Ruff, 2010) given its taxonomic uncertainty. Femoral head diameters are not available for the Burtele foot. To assess phalangeal robusticity, the diaphysis is modeled as a solid beam and the diaphyseal polar moment of area (J) calculated from the midshaft diameters using ellipse formulae (O'Neill and Ruff, 2004). Polar moments of area are compared to interarticular length since body mass estimates are unavailable for all of the Pliocene and Earlier Pleistocene pedal phalanges, except for A.L. 288-1y. The raw residuals from the reduced major axis line of the polar moment of area versus interarticular length for the recent human habitually unshod digits 2 to 5 sample are then compared ($\text{Ln J} = 4.243 \times \text{Ln length} - 8.43$, $r = 0.616$, $n = 171$).

Given that variable numbers of phalanges are available by individual, and that it is not always possible to reliably assign phalanges to a digit, SKX 16699 is compared to values for proximal phalanges from digits 2 to 5 individually. To avoid duplication by individual for the associated sets of phalanges, the comparisons employ repeated measure ANOVAs [calculations done with NCSS 8.0.16 (Hintze, 2012)]. Phalanx length is not different across the reference samples ($P = 0.453$), but the other comparisons are all significant at $P < 0.0001$.

3. Results

3.1. Phalangeal length

SKX 16699's interarticular length is 18.6 mm, which is shorter than those of 96.6% ($n = 179$) of the other fossil hominin pedal phalanges (Fig. 2A). It is among the smaller of the later *Homo* phalanges, and modestly longer than one of *H. naledi* (U.W. 101-1034). It falls well below those of BRT-VP-2/73, *Australopithecus afarensis*, *Australopithecus africanus* and *P. robustus*; among the australopiths, its length is approached only by those of A.L. 288-1y (21.0 mm), StW 355 (23.4 mm) and DNH-117 (22.2 mm).

When phalanx length is scaled to femoral head diameter as an index (Fig. 2B), the australopiths separate from the Late Pleistocene hominins. The smallest *Australopithecus afarensis* index (67.6) is for the A.L. 333-154 phalanx; the largest Late Pleistocene indices are for the Qafzeh 8 (65.2) and Veneri 2 (65.0) second phalanges. The StW 355 and DNH-117 phalanges, scaled against *Australopithecus africanus* and *P. robustus* mean femoral head diameters respectively, provide indices of 70.5 and 68.9, respectively, at the bottom of the *Australopithecus afarensis* range. The *H. naledi* indices fall among the relatively longer of the Late Pleistocene humans.

The values for SKX 16699 as a *P. robustus* (57.8) or an early *Homo* (45.5) bracket the interquartile ranges for Late Pleistocene *Homo* and are distinct from the australopith range. If the three shortest australopith phalanges (A.L. 288-1y, StW 355, DNH-117) are scaled to the smallest known femoral head diameters for their respective species (A.L. 288-1: 28.0 mm; Sts 14: ≈ 30.8 mm; SK 3121: 28.8 mm) and SKX 16699 is scaled to the smallest of them, assuming that they all derive from small individuals, their resultant indices are 78.6, 76.0, 77.1 and 66.4 respectively. Thus, SKX 16699 remains separate from the australopith specimens, if slightly above the highest later *Homo* values. SKX 16699 therefore has both an absolutely and, to the extent assessable, relatively short length, similar to those of *Homo*.

Comparing each phalanx length separately to each of the femoral head diameters within each taxonomic group (Table S2) modestly increases the ranges of indices for each sample or specimen. However, it does not change the overall pattern (Fig. S2), and the comparative samples remain significantly different from each other. The larger indices for SKX 16699 using *P. robustus* femoral head diameters overlap the smallest values for *Australopithecus afarensis*, StW 355 and DNH-117, but the majority of its indices using *P. robustus* femoral heads and all of the ones using early *Homo* values separate it from the australopith specimens.

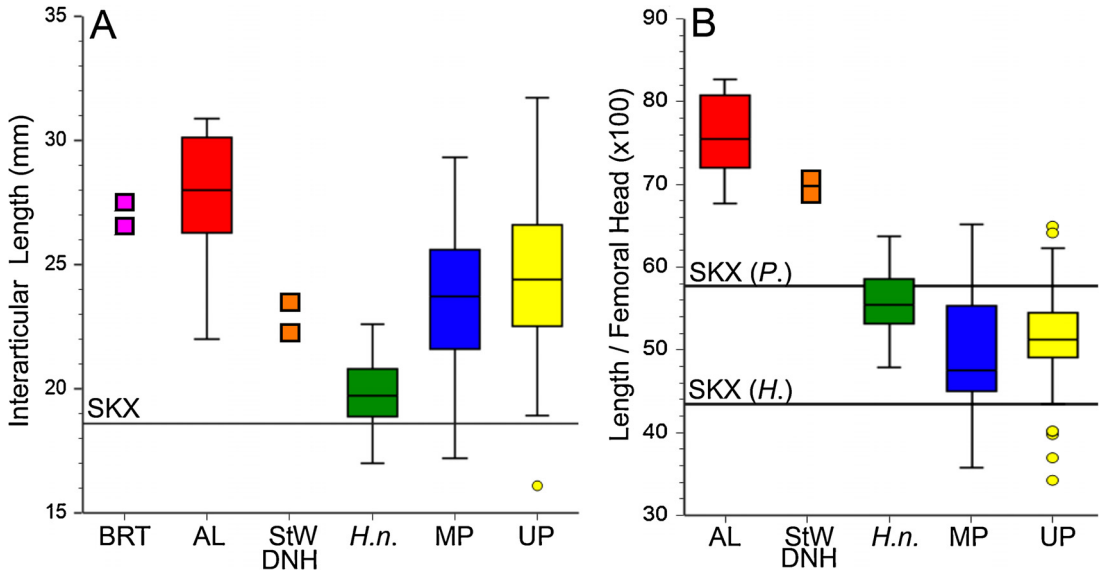

Fig. 2. Phalanx interarticular length (A) and interarticular length/femoral head diameter × 100 (B). Sample average femoral head diameters are employed for the australopith and *H. naledi* samples; see Fig. S2 for comparisons to individual values. SKX (*P.*) and SKX (*H.*) represent the values for SKX 16699 using *P. robustus* and early *Homo* average femoral head diameters, respectively. BRT: BRT-VP-2/73; AL: Hadar *Australopithecus afarensis*; StW: StW 355 *Australopithecus africanus*; DNH: DNH-117 *P. robustus* (StW 355 is above DNH-117 in both graphs); *H.n.*: *H. naledi*; MP: Middle Paleolithic humans; UP: Upper Paleolithic humans.

Fig. 2. Longueur interarticulaire de la phalange (A) et longueur phalangienne/diamètre de la tête fémorale × 100 (B). Les diamètres moyens de la tête fémorale sont utilisés pour les échantillons d'australopithèques et d'*H. naledi* ; voir Fig. S2 pour des comparaisons avec les valeurs individuelles. SKX (*P.*) et SKX (*H.*) représentent les valeurs pour SKX 16699 en utilisant les diamètres moyens de la tête fémorale pour *P. robustus* et pour *Homo* du début du Pléistocène. BRT : BRT-VP-2/73 ; AL : *Australopithecus afarensis* d'Hadar ; StW : *Australopithecus africanus* (StW 355) ; DNH : *P. robustus* (DNH-117) (StW 355 est au-dessus de DNH-117 dans les deux graphiques) ; *H.n.* : *H. naledi* ; MP : hommes du Paléolithique moyen ; UP : hommes du Paléolithique supérieur.

3.2. Diaphyseal robusticity

The robusticity of the SKX 16699 diaphysis is assessed by comparing its midshaft polar moment of area (modeled as a solid beam) to those of the other hominin fossil samples (Fig. 3A). The two Late Pleistocene samples follow the pattern of habitually unshod and shod recent humans (Middle and Upper Paleolithic remains, respectively) (Trinkaus, 2005). The *Australopithecus afarensis* phalanges (including the small A.L. 288-1y) and the two phalanges from BRT-VP-2/73 fall along the gracile margin of the habitually shod human sample. Their phalangeal "gracility" is likely a result of their phalangeal lengths, given that they are relatively long and australopith postcrania are otherwise robust (Ruff et al., 1999). The *H. naledi* phalanges align with the Middle Paleolithic sample. The two later australopith phalanges, StW 355 and DNH-117, are close to the *H. naledi* phalanges and among the Late Pleistocene ones. SKX 16699 is within the range of both the Middle and Upper Paleolithic samples, close to those of *H. naledi*, distinct from the *Australopithecus afarensis* ones, yet in line with the two later australopiths from South Africa (StW 355 and DNH-117).

The distributions of their residuals from a recent human unshod sample line (Fig. 3B) places SKX 16699 between the medians of the two later *Homo* phalanx samples and among the more gracile of the *H. naledi* and Middle Paleolithic phalanges. It is similar to the values for the two later South African australopith specimens, above the Burtele values, and well separated from the *Australopithecus afarensis* sample. It is unclear to what extent the differences in earlier hominin phalangeal robustness are driven by shaft diameters versus length (Fig. 2); the similarity of SKX 16699 to StW 355 and DNH-117 may be due in part to their modest lengths, yet A.L. 288-1y remains gracile along with the other *Australopithecus afarensis* phalanges.

3.3. Diaphyseal curvature

The dorsal contour of SKX 16699 in lateral view exhibits a modest convexity, one that is evenly distributed proximodistally along the diaphysis (Fig. 1); its plantar contour is only slightly concave. It is therefore more curved dorsally than are those of most Late Pleistocene and recent humans, which have a straight or slightly convex dorsal diaphyseal profile (Fig. 4). Yet, its dorsal curvature is substantially less than those of *Australopithecus afarensis, Australopithecus africanus* and BRT-VP-2/73 (Fig. 4; cf. Haile-Selassie et al., 2012; Latimer et al., 1982; Ward et al., 2012). It is similar to those of the *H. naledi* phalanges, despite their phalanges being described as having "significantly greater curvature than those of modern humans" (Harcourt-Smith et al., 2015:4). Yet, the slight plantar concavity of SKX 16699 closely resembles those of later *Homo* phalanges and is close to those of the *H. naledi* phalanges. It contrasts with the distinctly plantarly concave proximal phalanges of *Australopithecus afarensis*, StW 355 and DNH-117 (Fig. 4; cf. Latimer et al., 1982; Vernon, 2013; Ward et al., 2012).

Susman et al. (2001) provided an "included angle" of 22° for SKX 16699, a measure of its midline curvature and hence one that combines both the dorsal convexity and the

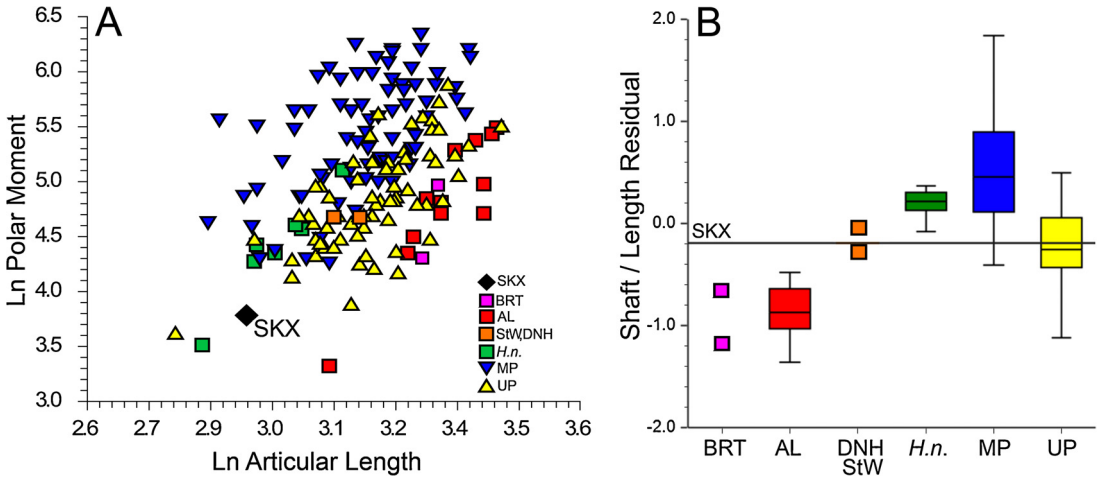

Fig. 3. Bivariate plot of the midshaft ln polar moment of area (modeled as a solid beam) versus ln interarticular length for SKX 16699 and comparative lateral proximal pedal phalanges 2 to 5 (A). Boxplot of the residuals from reduced major axis line through the recent human habitually unshod sample (B). The very short phlanages in A are U.W. 101-1034 and from the Shanidar 4 and 8 and Continenza 1 fifth digits. Abbreviations as in Fig. 2.
Fig. 3. Distribution bivariée du moment polaire In de la diaphyse (représentée comme un fasiceau solide) en fonction de la longueur articulaire In de SKX 16699 et des phalanges latérales proximales d'échantillons de comparaison 2 à 5 (A) et *boxplot* pour les résiduels à partir de la ligne de régression d'axe majeur sur un échantillon d hommes récents, habituellement non chaussés (B). Les phalanges très courtes en A sont U.W. 101-1034 et proviennent des cinquièmes orteils de Continenza 1 et de Shanidar 4 et 8. Voir les abréviations en Fig. 2.

degree of dorsoplantar expansion of the proximal diaphysis (Stern et al., 1995; Susman et al., 1984). This angle is substantially below the value of 36° for both A.L. 288-1y and StW 355, which are similar to other *Australopithecus afarensis* proximal pedal phalanges, but among the more curved of a recent human sample (Susman et al., 1984, 2001). Yet, the diaphysis of SKX 16699 expands more proximally than do those of *Australopithecus* (albeit not as much as some later *Homo* phalanges) (Fig. 4), such that the "included angle" likely minimizes the difference in dorsal curvature between it and those of *Australopithecus*. SKX 16699 also contrasts with DNH-117, whose curvature is similar to StW 355 and the *Australopithecus afarensis* phalanges (Vernon, 2013).

3.4. Flexor sheath attachments

Hominin pedal phalanges have variably developed medial and lateral sulci, with or without small crests, for the attachments of the flexor digitorum longus and brevis muscles' fibrous sheaths. The sulci extend from the proximal metatarsophalangeal capsular attachment to an area close to the distal trochlea. In later Pleistocene humans, they are marked, sometimes with small crests, on the proximal-to-middle shaft and in the dorsoplantar middle of the medial and lateral diaphysis (Fig. 4). On the *Australopithecus afarensis* and StW 355 phalanges (Fig. 4; cf. Ward et al., 2012), they are variably evident along the full diaphysis and are more developed on the distal half to two-thirds of the diaphysis. Their sulci are commonly bordered medially and laterally by small crests extending along the middle to distal diaphysis, located medioplantarly and lateroplantarly as opposed to the more directly medial and lateral positions of midshaft crests on later *Homo* diaphyses. The DNH-117 phalanx resembles the earlier *Australopithecus* ones in this respect. The *H. naledi* configurations are similar to the pattern seen in later *Homo*.

The fibrous flexor sheath attachments of SKX 16699 (Fig. 1) resemble those of Late Pleistocene *Homo* and *H. naledi*; they are distinct only on the proximal two-thirds of the diaphysis with the deepest portions of the sulci and the associated medial and lateral projections centered approximately one-third of the distance from the proximal epiphysis. The rounded crests are dorsoplantarly located mid-medial and mid-lateral.

3.5. Flexor sheath diaphyseal expansion

As a result of the more distal development of the fibrous sheath attachments on *Australopithecus* pedal phalanges, the widest portions of most of their diaphyses are the distal halves and the narrowest points are close to the proximal epiphysis (Fig. 4). The exceptions are A.L. 333-168 and DNH-117, which have largely parallel medial and lateral diaphyseal margins (Vernon, 2013; Ward et al., 2012). The *H. naledi* phalanges largely have a midshaft bulge for the flexor sheath crests, with similar mediolateral constrictions proximal and distal of the crests. Later *Homo* pedal proximal phalanges, in contrast, have the narrow portion of the diaphysis either at midshaft or towards the distal shaft (Fig. 4). SKX 16699 has its narrowest portion slightly distal of midshaft, thereby giving it an "hour-glass" profile (Susman et al., 2001).

3.6. Metatarsal facet orientation

Investigations of the orientation of the metatarsal facet on early hominin lateral proximal pedal phalanges (Duncan et al., 1994; Fernández, 2016; Haile-Selassie et al., 2012; Latimer and Lovejoy, 1990; Susman et al., 1984; Vernon,

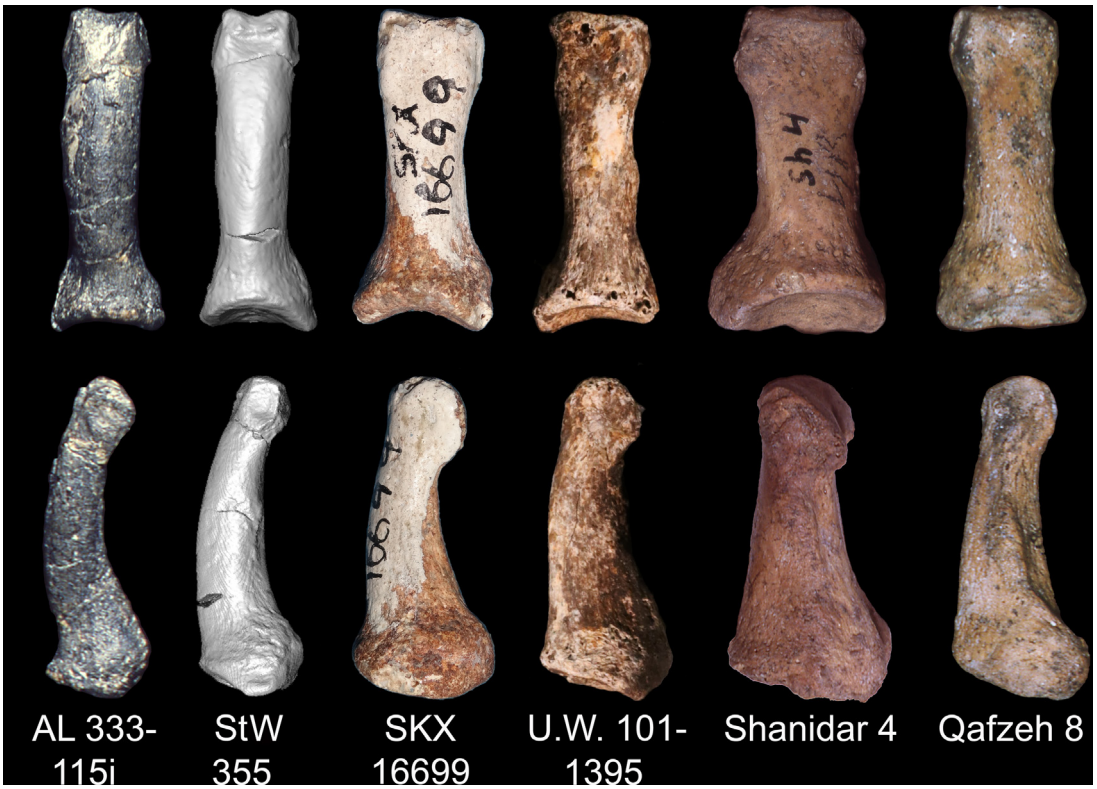

Fig. 4. Comparisons of the SKX 16699 right proximal pedal phalanx in dorsal (above) and lateral (below) views to the A.L. 333-115i *Australopithecus afarensis* (left reversed), StW 355 *Australopithecus africanus*, U.W. 101-1395 *H. naledi* (left reversed), the Shanidar 4 late archaic human, and the Qafzeh 8 Middle Paleolithic modern human proximal pedal phalanges. The phalanges are scaled to the same length. The fourth proximal phalanges of the associated A.L. 333-115, Shanidar 4 and Qafzeh 8 are shown, since they represent an average for the digit attribution of SKX 16699. The others are isolated specimens and cannot be assigned to digit with absolute certainty. The A.L. 333-115i images are from B. Latimer/Cleveland Museum of Natural History, and the U.W. 101-1395 images are from W.E.H. Harcourt-Smith.

Fig. 4. Phalange proximale droite du pied de SKX 16699 en vues dorsale (en haut) et latérale (en bas), comparée aux phalanges d'*Australopithecus afarensis* (A.L. 333-115i ; gauche retournée), d'*Australopithecus africanus* (StW 355), de *H. naledi* (U.W. 101-1395 ; gauche retournée), d'un Néandertalien (Shanidar 4), et d'un homme moderne du Paléolithique moyen (Qafzeh 8). Les quatrièmes phalanges proximales de A.L. 333-115, Shanidar 4 et Qafzeh 8 sont figurées, puisqu'elles proviennent du même orteil dont la moyenne a permis l'identification de SKX 16699 ; les autres phalanges, qui sont des specimens isolés, ne peuvent pas être associées avec une certitude absolue à un orteil latéral spécifique. Les photos de A.L. 333-115i proviennent de B. Latimer/Cleveland Museum of Natural History, et celles de U.W. 101-1395 sont de W.E.H. Harcourt-Smith.

2013; Ward et al., 2012) have noted the predominantly proximodorsal orientation of the proximal phalangeal facet (or 'dorsal canting'), and these observations are combined with metatarsal indications of some degree of metatarsophalangeal dorsiflexion (Latimer and Lovejoy, 1990; Zipfel et al., 2009). On the proximal phalanges, assessment of the angle between the mid-facet tangent and the articular axis (the articular angle; Fig. 5) shows that the BRT-VP-2/73, StW 355 and most of the *Australopithecus afarensis* facets (the angle is not available for DNH-117) are angled slightly dorsal of directly proximal, with the more angled of the phalanges minimally overlapping the range of variation of the Late Pleistocene humans. The habitually unshod human sample has slightly higher angles than the habitually shod one ($P = 0.102$) (cf. Griffin and Richmond, 2010). The *H. naledi* sample exhibits angles well within the later *Homo* range. The SKX 16699 phalanx, with an angle of 110°, is among the more angled of the later Pleistocene humans. It is distinct from the earlier hominin range and above the values for the *H. naledi* sample.

3.7. Medial and lateral base projections

In lateral view, the medial and lateral sides of the phalangeal base (i.e., proximal epiphysis) of Late Pleistocene and recent humans project most proximally at the plantar articular margin because the collateral (and plantar) metatarsophalangeal ligaments insert plantarly on the phalanx (Martin, 2011). The epiphyses of BRT-VP-2/73 and *Australopithecus* project proximally near the dorsoplantar middles of articulations (Fig. 4; cf. Haile-Selassie et al., 2012; Latimer et al., 1982; Susman et al., 1984; Ward et al., 2012), whereas that of DNH-117 has the proximal projection slightly plantar of the dorsoplantar middle of the base (Vernon, 2013). In this feature, SKX 16699 is intermediate between *Australopithecus* and later *Homo* phalanges, in that its proximal projection is ≈ 35% of the dorsoplantar distance from the plantar margin [assessed on the medial side (Fig. 1) to avoid the plantar growth]. The *H. naledi* phalanges are mostly damaged on the sides of their bases, but they (e.g., U.W. 101-1395) appear to exhibit a pattern closer to that of later Pleistocene humans.

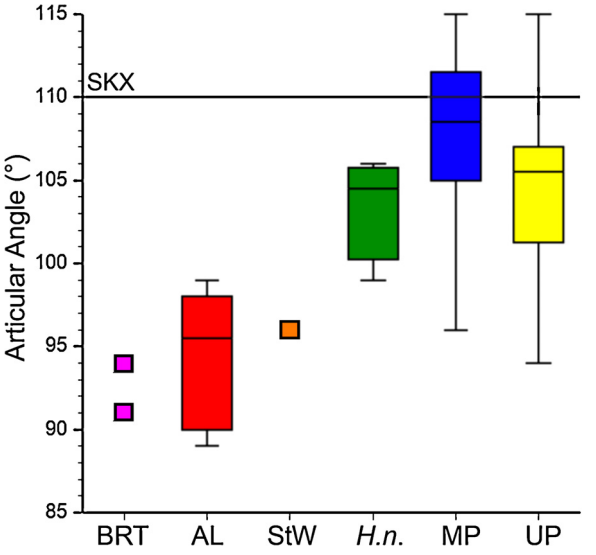

Fig. 5. Boxplot of the angles between the articular axis and mid-sagittal tangent to the metatarsal facet ('articular angle') for SKX 16699 (110°) and the comparative samples. Abbreviations as in Fig. 2.
Fig. 5. *Boxplot* des angles entre l'axe interarticulaire et la tangente dorso-plantaire à la facette métatarsienne (« angle articulaire ») pour SKX 16699 (110°) et les échantillons fossiles de comparaison. Voir les abréviations en Fig. 2.

4. Discussion

The SKX 16699 lateral pedal proximal phalanx from the initial Pleistocene of Swartkrans provides a morphological pattern generally similar to those of Late Pleistocene (and recent) humans. This morphology contrasts those of pedal phalanges attributed to *Australopithecus* and *Paranthropus*, which are more similar to the phalanges of *Ardipithecus* and the Burtele foot. The SKX 16699 affinities are reflected in the minimal curvature of its plantar diaphyseal contour, the modest development and mid-to-proximal position of the flexor sheath attachments, the consequent mid-to-distal shaft mediolateral constriction, the flexor sheath crests in the dorsoplantar middle of the diaphysis, and the distinctly dorsal slope of its metatarsal facet. The dorsal shaft curvature of SKX 16699 is greater than is normally present in recent *Homo* pedal phalanges, but less marked than those of *Australopithecus* phalanges, and the proximal collateral ligament insertions are intermediate between the dorsoplantar middle position of *Australopithecus* and the plantar position of later *Homo*. In addition, it is the shortest of the Pliocene/Early Pleistocene pedal lateral proximal phalanges. Although its absolutely short length is approached by three fossil specimens, it remains relatively short when scaled with proxies for body size (e.g., known or probable femoral head diameters). Its diaphyseal robustness, scaled to phalanx length, is among the range of *Homo* specimens, distinct from the *Australopithecus afarensis* pedal phalanges, but close to StW 355 and DNH-117. Therefore, although SKX 16699 does not conform entirely to the Late Pleistocene and recent human morphological pattern, it is markedly distinct from the phalanges of *Australopithecus afarensis* and *Australopithecus africanus* and largely separate from the one attributed to *P. robustus*. Among all the fossils studied here, SKX 16699 resembles the proximal pedal phalanges of the Dinaledi sample in most of these features. Accordingly, its morphology indicates a lateral forefoot that should have functioned in a manner similar to those of recent unshod humans.

Although the basic structure of the human tarsometatarsal pedal skeleton had emerged by the Early-to-Mid Pliocene in *Australopithecus*, various morphological differences with later Pleistocene and recent human pedal elements existed. In particular, australopiths, and to a lesser extent early *Homo*, exhibit first metatarsal heads capable of greater hallucal mobility (Pontzer et al., 2010; Susman, 1989; Susman and de Ruiter, 2004) and non-hallucal metatarsal heads mostly suggest less habitual ranges of dorsiflexion than is common in later *Homo* (DeSilva et al., 2012; Susman et al., 1984; Zipfel et al., 2009). It is possible that the configuration of the SKX 16699 proximal epiphysis, with mid-plantar collateral ligament insertions, is related to these minor differences in the distal metatarsals of the lateral toes. The combination of features evident in SKX 16699, albeit in the pedal context of an australopith or early *Homo* tarsometatarsal and hallucal skeleton, could provide the earliest evidence for the distinctly human pattern of lateral forefoot function, one related to increasing substrate traction (Stott et al., 1973), running performance (Rolian et al., 2009), and tightening the plantar aponeurosis in a foot with pedal arches (Hicks, 1954). If so, it is at about the same time as the relatively short intermediate phalanges of KNM-ER 803, as well as the oldest evidence for a functional pattern in the more proximal lower limb similar to those of Middle and Late Pleistocene archaic *Homo* (Day and Leakey, 1974; Pontzer et al., 2010; Rose, 1984; Trinkaus, 1984). Confirmation of this hypothesis will require at least an articulated set of metatarsals and phalanges, but the derived "human" features of this isolated phalanx are difficult to understand otherwise.

Member 1 of Swartkrans has yielded craniodental fossil remains of both *P. robustus* and early *Homo* (Grine, 1989), thereby preventing a confident attribution of the unassociated SKX 16699 specimen to either taxon. But because its morphology contrasts with the DNH-117 phalanx attributed to *P. robustus* (Vernon, 2013) in most features, and it is close to those of *H. naledi* and, to a lesser extent, of later *Homo*, it is tempting to assign SKX 16699 to early *Homo*. But better craniodental and postcranial associations are needed from Member 1 of Swartkrans to test this inference.

5. Conclusion

The re-assessment of the initial Early Pleistocene hominin lateral toe phalanx from Member 1 of Swartkrans Cave, SKX 16699, confirms and expands upon the initial assessments, which placed it morphologically close to later Pleistocene and recent humans. This affinity is evident in its short length and robust diaphysis, but it is especially apparent in its patterns of diaphyseal curvature, flexor sheath attachments, "hour-glass" contour and metatarsal

facet orientation. As such it may provide the earliest evidence for the derived human pattern of lateral forefoot function, whatever morphofunctional mosaic may have been present in the individual's tarsometatarsal and hallucal remains.

Acknowledgments

S. Potze (Ditsong National Museum of Natural History) and B. Zipfel (Evolutionary Studies Institute, University of the Witwatersrand) kindly facilitated the study the original SKX 16699 and StW 355 fossils. Copies of micro-CT scans of SKX 16699 and StW 355 were generously shared by T. Jashashvili. W. Harcourt-Smith provided images of Dinaledi phalanges, J.M. DeSilva provided the Dinaledi femoral head diameters, and B. Latimer provided images of A.L. 333-115. W. Harcourt-Smith and J.M. DeSilva provided helpful comments on an earlier verion. F. Mallegni furnished the Italian Upper Paleolithic measurements, and A. Soficaru provided the von Gaál (1928) reference. Portions of the data collection were supported by the Leakey, Wenner-Gren and National Science Foundations (to ET) and National Science Foundation (BCS 1317047) (to BAP). To all we are immensely grateful.

Appendix A. Supplementary data

Supplementary data associated with this article can be found, in the online version, at http://dx.doi.org/10.1016/j.crpv.2016.07.003.

References

Auerbach, B.M., Ruff, C.B., 2004. Human body mass estimation: a comparison of "morphometric" and "mechanical" methods. Am. J. Phys. Anthropol. 125, 331–342.

Balter, V., Blichert-Toft, J., Braga, J., Telouk, P., Thackeray, F., Albarède, F., 2008. U-Pb dating of fossil enamel from the Swartkrans Pleistocene hominid site, South Africa. Earth Planet. Sci. Lett. 267, 236–246.

Crompton, R.H., Pataky, T.C., Savage, R., D'Août, K., Bennett, M.R., Day, M.H., Bates, K., Morse, S., Sellers, W.I., 2012. Human-like external function of the foot, and fully upright gait, confirmed in the 3.66 million year old *Laetoli hominin* footprints by topographic statistics, experimental footprint-formation and computer simulation. J. Roy. Soc. Interf. 9 (69), 707–719.

Day, M.H., Leakey, R.E.F., 1974. New evidence of the genus *Homo* from East Rudolf, Kenya (III). Am. J. Phys. Anthropol. 41, 367–380.

Dembo, M., Radovčić, D., Garvin, H.M., Laird, M.F., Schroeder, L., Scott, J.E., Brophy, J., Ackermann, R.R., Musiba, C.M., de Ruiter, D.J., Moores, A.Ø., Collard, M., 2016. The evolutionary relationships and age of *Homo naledi*: an asessment using dated Bayesian phylogenetic methods. J. Hum. Evol. 97, 17–26.

DeSilva, J.M., Proctor, D.J., Zipfel, B., 2012. A complete second metatarsal (StW 89) from Sterkfontein Member 4, South Africa. J. Hum. Evol. 63, 487–496.

DeSilva, J.M., Holt, K.G., Churchill, S.E., Carlson, K.J., Walker, C.S., Zipfel, B., Berger, L.R., 2013. The lower limb and mechanics of walking in *Australopithecus sediba*. Science 340 (6129), 1232999e1–1232999e5.

Duncan, A.S., Kappelman, J., Shapiro, L.J., 1994. Metatarsophalangeal joint function and positional behavior in *Australopithecus afarensis*. Am. J. Phys. Anthropol. 93, 67–81.

Fernández, P.J., (Ph.D. Dissertation) 2016. Form and function of the anthropoid forefoot. Stony Brook University.

Grabowski, M., Hatala, K.G., Jungers, W.L., Richmond, B.G., 2015. Body mass estimates of hominin fossils and the evolution of human body size. J. Hum. Evol. 85, 75–93.

Griffin, N.L., Richmond, B.G., 2010. Joint orientation and function in great ape and human proximal pedal phalanges. Am. J. Phys. Anthropol. 141, 116–123.

Grine, F.E., 1989. New hominid fossils from the Swartkrans Formation (1979–1986 excavations): Craniodental specimens. Am. J Phys. Anthropol. 79, 409–449.

Haile-Selassie, Y., Saylor, B.Z., Deino, A., Levin, N.E., Alene, M., Latimer, B.M., 2012. A new hominin foot from Ethiopia shows multiple Pliocene bipedal adaptations. Nature 483, 565–570.

Harcourt-Smith, W.E.H., Throckmorton, Z., Congdon, K.A., Zipfel, B., Deane, A.S., Drapeau, M.S.M., Churchill, S.E., Berger, L.R., DeSilva, J.M., 2015. The foot of *Homo naledi*. Nature Comm, http://dx.doi.org/10.1038/ncomms9432.

Hatala, K.G., Demes, B., Richmond, B.G., 2016. Laetoli footprints reveal bipedal gait biomechanics different from those of modern humans and chimpanzees. Proc. Roy. Soc. (283B, 20160235).

Hicks, J.H., 1954. The mechanics of the foot II. The plantar aponeurosis and the arch. J. Anat. (Lond.) 88, 25–30.

Hintze, J., 2012. NCSS 8. NCSS, LLC, Kaysville UT.

Latimer, B., Lovejoy, C.O., 1990. Metatarsophalangeal joints of *Australopithecus afarensis*. Am. J. Phys. Anthropol. 83, 13–23.

Latimer, B.L., Lovejoy, C.O., Johanson, D.C., Coppens, Y., 1982. Hominid tarsal, metatarsal, and phalangeal bones recovered from the Hadar Formation: 1974–1977 collections. Am. J. Phys. Anthropol. 57, 701–719.

Lorenzo, C., Arsuaga, J.L., Carretero, J.M., 1999. Hand and foot remains from the Gran Dolina Early Pleistocene site (Sierra de Atapuerca, Spain). J. Hum. Evol. 37, 501–522.

Lovejoy, C.O., Latimer, B., Suwa, G., Asfaw, B., White, T.D., 2009. Combining prehension and propulsion: the foot of *Ardipithecus ramidus*. Science 326, 72e8, http://dx.doi.org/10.1126/science.1175832.

Marchi, D., Walker, C.S., Wei, P., Holliday, T.W., Churchill, S.E., Berger, L.R., DeSilva, J.M., 2016. The thigh and leg of *Homo naledi*. J. Hum. Evol. (in press).

Martin, R.L., 2011. The ankle and foot complex. In: Levangie, P.K., Norkin, C.C. (Eds.), Joint structure and function, 5th ed. F.A. Davis, Philadelphia, pp. 440–481.

O'Neill, M.C., Ruff, C.B., 2004. Estimating human long bone cross-sectional geometric properties: a comparison of noninvasive methods. J. Hum. Evol. 47, 221–235.

Pablos, A., Pantoja, A., Martínez, I., Lorenzo, C., Arsuaga, J.L., 2015. Metric and morphological analysis of the foot in the Middle Pleistocene sample of Sima de los Huesos (Sierra de Atapuerca, Burgos, Spain). Quatern. Int., http://dx.doi.org/10.1016/j.quaint.2015.08.044.

Pontzer, H., Rolian, C., Rightmire, G.P., Jashashvili, T., Ponce de León, M., Lordkipanidze, D., Zollikofer, C.P.E., 2010. Locomotor anatomy and biomechanics of the Dmanisi hominins. J. Hum. Evol. 58, 492–504.

Raichlen, D.A., Gordon, A.D., Harcourt-Smith, W.E.H., Foster, A.D., Haas, W.R., 2010. Laetoli footprints preserve earliest direct evidence of human-like bipedal biomechanics. PloS One 5 (3), e9769.

Rolian, C., Lieberman, D.E., Hamill, J., Scott, J.W., Werbel, W., 2009. Walking, running and the evolution of short toes in humans. J. Exp. Biol. 212, 713–721.

Rose, M.D., 1984. A hominine hip bone, KNM-ER 3228, from East Late Turkana, Kenya. Am. J. Phys. Anthropol. 63, 371–378.

Ruff, C.B., 2010. Body size and body shape in early hominins–implications of the Gona Pelvis. J. Hum. Evol. 58, 166–178.

Ruff, C.B., McHenry, H.M., Thackeray, J.F., 1999. Cross-sectional morphology of the SK 82 and 97 proximal femora. Am. J. Phys. Anthropol. 109, 509–521.

Stern Jr., J.T., Jungers, W.L., Susman, R.L., 1995. Quantifying phalangeal curvature: an empirical comparison of alternative methods. Am. J. Phys. Anthropol. 97, 1–10.

Stott, J.R.R., Hutton, W.C., Stokes, I.A.F., 1973. Forces under the foot. J. Bone Joint Surg. 55B, 335–344.

Susman, R.L., 1989. New hominid fossils from the Swartkrans Formasion (1979–1986 excavations): postcranial specimens. Am. J. Phys. Anthropol. 79, 451–474.

Susman, R.L., de Ruiter, D., 2004. New hominin first metatarsal (SK 1813) from Swartkrans. J. Hum. Evol. 47, 171–181.

Susman, R.L., Stern Jr., J.T., Jungers, W.L., 1984. Arboreality and bipedality in the Hadar hominids. Folia Primat. 43, 113–156.

Susman, R.L., de Ruiter, D., Brain, C.K., 2001. Recently identified postcranial remains of *Paranthropus* and early *Homo* from Swartkrans Cave, South Africa. J. Hum. Evol. 41, 607–629.

Trinkaus, E., 1983. The Shanidar Neandertals. Academic Press, New York.

Trinkaus, E., 1984. Does KNM-ER 1481A establish *Homo erectus* at 2.0 myr BP? Am. J. Phys. Anthropol. 64, 137–139.
Trinkaus, E., 2005. Anatomical evidence for the antiquity of human footwear use. J. Archaeol. Sci. 32, 1515–1526.
Vernon, D.S., (Masters Thesis) 2013. A morphometric analysis of the phalanges and a fragmentary first metatarsal from the Drimolen hominin site, South Africa. University of Johannesburg.
Ward, C.V., 2013. Postural and locomotor adaptations of *Australopithecus* species. In: Reed, K.E., Fleagle, J.G., Leakey, R.E. (Eds.), The Paleobiology of *Australopithecus*. Springer, New York, pp. 235–245.
Ward, C.V., Kimbel, W.H., Harmon, E.H., Johanson, D.C., 2012. New postcranial fossils of *Australopithecus afarensis* from Hadar, Ethiopia (1990–2007). J. Hum. Evol. 63, 1–51.
White, T.D., Suwa, G., 1987. Footprints at Leotoli: facts and interpretations. Am. J. Phys. Anthropol. 72, 485–514.
Zipfel, B., DeSilva, J.M., Kidd, R.S., 2009. Earliest complete hominin fifth metatarsal – implications for the evolution of the lateral column of the foot. Am. J. Phys. Anthropol. 140, 532–545.